Available online at www.sciencedirect.com
SCIENCE DIRECT®
Polymer 44 (2003) 7729–7738
polymer
www.elsevier.com/locate/polymer

The effect of ionic cross-links on the deformation behavior of homoblends made of poly(styrene-*co*-styrenesulfonic acid) and poly(styrene-*co*-4-vinylpyridine)

Wenjie Chen, J.A. Sauer, Masanori Hara*

Department of Chemical and Biochemical Engineering, Rutgers University, 98 Brett Road, Piscataway, NJ 08854-8058, USA

Received 17 June 2003; received in revised form 12 September 2003; accepted 15 September 2003

Abstract

Deformation behavior of stoichiometric blends made from poly(styrene-*co*-styrenesulfonic acid) (SPS) and poly(styrene-*co*-4-vinylpyridine) (SVP) was investigated by TEM observation of strained thin films. An FTIR investigation revealed that ionic cross-links were formed between the component polymers upon blending due to intermolecular ion–ion interactions, which arose from proton transfer from sulfonic acid groups to pyridine groups. TEM observations indicate that the deformation mode of the blends changed from crazing only to crazing plus shear deformation, with the shear contribution becoming larger, as the ion content in the blends increased. Such changes in deformation mode can be understood as arising from an increase in the 'effective' strand density due to the formation of ionic cross-links upon blending. It was also found that the ionic cross-links via pyridinium cation/sulfonate anion ion pairs were more effective in inducing the transition of deformation mode than ionic cross-links via $-SO_3^-/Na^+$ or $-SO_3^-/Ca^{2+}$ ion pairs.

Keywords: Ionic cross-links; homoblends; deformation modes

1. Introduction

Deformation behavior of amorphous glassy polymers has been studied extensively over the years [1–3]. It is well known that two deformation modes, shear yielding and crazing, may be observed when thin films of amorphous glassy polymers like polystyrene (PS) and polycarbonate (PC) are strained in tension. Shear yielding takes place in either highly localized shear bands or diffuse shear deformation zones. No volume change occurs in these zones. Crazes consist of many small oriented fibrils, with diameter in the range of 5–30 nm, interspersed with voids. Unlike shear yielding, crazing is a cavitational process, leading to an increase in volume. Brittle polymers, such as PS, usually deform by crazing, while more ductile polymers, such as PC, usually deform by shear yielding. Although crazes are load bearing and extensive crazing can be beneficial for improving toughness, as seen in rubber-toughened polymers [1,4], in glassy polymers cracks can propagate readily through crazes by breakdown of the fibril structure and therefore decrease fracture resistance. Thus, one way to make polymers more fracture resistant is to control crack nucleation and growth in crazes by suppressing crazing in favor of shear deformation.

It is now well recognized that the *entanglement* strand density, ν_e, of glassy polymers plays an important role in large-strain behavior, such as deformation and fracture [1–3,5]. Here, the polymer is perceived at temperature well below T_g as a network structure due to entanglements. The (entanglement) strand is defined as a chain segment bounded by physical entanglements and the strand density is the number of strands per unit volume. As the entanglement density, ν_e, rises, the crazing stress increases, but the shear yield stress, and hence shear deformation, is little influenced by the value of ν_e [3]. Thus an increase in ν_e leads to suppression of crazing in favor of shear deformation. For thin films of a series of homopolymers, copolymers, and miscible polymer blends, in which ν_e values ranged from 1×0^{25} to 30×10^{25} chains/m^3, the deformation behavior was found to vary systematically with ν_e [3,5]. For polymers with $\nu_e < 4 \times 0^{25}$ chains/m^3, as typically found for PS, only crazing was observed and strain to fracture was low. For polymers with ν_e between 4×10^{25}

* Corresponding author. Tel.: +1-732-445-3817; fax: +1-732-445-2581.
E-mail address: mhara@rci.rutgers.edu (M. Hara).

0032-3861/$ - see front matter © 2003 Elsevier Ltd. All rights reserved.
doi:10.1016/j.polymer.2003.09.053

and 8×10^{25} chains/m^3, as seen for poly(styrene-*co*-acrylonitrile), both crazes and shear deformation zones in competition were observed. For polymers with $\nu_e > 8 \times 10^{25}$ chains/m^3, as seen for PC, only shear deformation zones were observed and the material was ductile. The change of the deformation mode from crazing (which involves micro-fibril formation) to shear deformation (which does not) with increase of strand density can be rationalized as arising from the increase of energy required to break more main-chain bonds during formation of fibril surfaces [2].

It was found by Kramer and co-workers [3,5] that introducing *covalent cross-links* into PS raised the effective strand density, thereby suppressing crazing: the deformation mode changed from crazing only to crazing plus shear deformation and then shear deformation only as the degree of cross-linking increased. The total strand density, ν, in covalently cross-linked polymers is the sum of the entanglement strand density ν_e and the covalent cross-link strand density ν_x: i.e. $\nu = \nu_e + \nu_x$. Thus, craze suppression by cross-linking presents a potentially useful method for improving fracture properties.

The concept of strand density has been extended by Hara and co-workers to include the effect of *ionic cross-links* observed in ionomers [6–9]. Ionomers contain ionic groups of up to 10–15 mol% along hydrocarbon backbone chains. Because of the difference in polarity between ionic groups and hydrocarbon chains, there is a strong electrostatic driving force toward aggregation of the ionic groups. Two types of aggregates, multiplets and clusters, have been suggested to exist in ionomers, as proposed by Eisenberg [10]. A multiplet is defined as an aggregate in which ions are in contact with each other with no intervening hydrocarbon chains. A cluster is an aggregate of multiplets and contains some hydrocarbon chains. These aggregates also function as ionic cross-links, which is evidenced by an increase in T_g with ion content. Therefore, the total strand density in ionomers includes the contribution from ionic cross-links in addition to that from physical entanglements of the base polymer.

It has been found that the introduction of ionic groups into PS or PMMA, i.e. formation of sulfonated PS (SPS) or PMMA-based ionomers, can alter the deformation mechanisms in strained thin films [6–9]. For instance, for SPS ionomers with sodium as the counterion, a transmission electron microscopy (TEM) study of strained thin films revealed that the deformation mode changed from straight, long crazes, to shorter and branched crazes and then to crazing plus shear deformation, when the ion content increased. These changes of deformation behavior can be understood as arising from an increased *effective* strand density due to ionic cross-linking. The change in the deformation mode is translated into changes in bulk mechanical properties. For example, both the tensile strength and the tensile toughness (energy to fracture) are increased significantly as the ion content is increased [6,9]. Since ionic cross-links are thermolabile and their introduction will not lead to the loss of melt processability of the materials, the introduction of ionic cross-links may provide a more practical method to enhance mechanical properties of glassy polymers as compared with the incorporation of covalent cross-links.

In contrast to ionic cross-links that are formed through the aggregation of ion pairs as seen for SPS ionomers or PMMA-based ionomers, ionic cross-links can be introduced to polymers directly via intermolecular ionic bonding. Such a method has been applied to enhance miscibility of otherwise immiscible polymer pairs [11–15]. For example, PS is immiscible with poly(ethyl acrylate). However, when PS is lightly sulfonated and mixed with a copolymer, poly(ethyl acrylate-*co*-4-vinylpyridine), the blend shows a single glass transition at functional group contents of 4 mol% or higher [11]. The driving force for the miscibility enhancement is the electrostatic attractive interaction between the pyridinium cation and sulfonate anion, which are produced by proton transfer from sulfonic acid groups to pyridine groups. The formation of an ion pair between pyridinium cation and sulfonate anion then can directly lead to the formation of ionic cross-links between polymer chains. The ionic interaction is expected to be stronger via such direct ion pair formation than via ionic aggregate formation, as typically seen in the SPS ionomer [16]. Despite this advantage, little work has been conducted on the effect of ion–ion type ionic bonds on the deformation behavior and mechanical properties of polymer blends. Hence, it is of interest to study the effect of intermolecular ionic cross-links via pyridinium cation and sulfonate anion on the mechanical properties of polymer blends. As a model blend system, we have studied homoblends made of poly(styrene-*co*-styrenesulfonic acid) (SPS) and poly(styrene-*co*-4-vinylpyridine) (SVP) containing stoichiometric amount of sulfonic acid and pyridine groups. The only difference between this homoblend and PS is the presence of interacting groups (see Fig. 1). By using this simple model system, we can obtain direct information about the effect of intermolecular ionic cross-links on the deformation behavior of the base polymer. In this study, ion–ion interactions were characterized by FTIR; and the deformation behavior of the SPS/SVP blends, with different interacting group contents, was investigated by TEM of strained thin films. The results will be discussed in terms of the concept of an existing strand density that includes ionic strand density via ionic cross-links, in addition to entanglement strand density.

2. Experimental

2.1. Materials

Sulfonated polystyrene (SPS) was prepared by sulfonation of polystyrene with a sulfonating agent, acetyl sulfate, according to the procedure described by Makowski

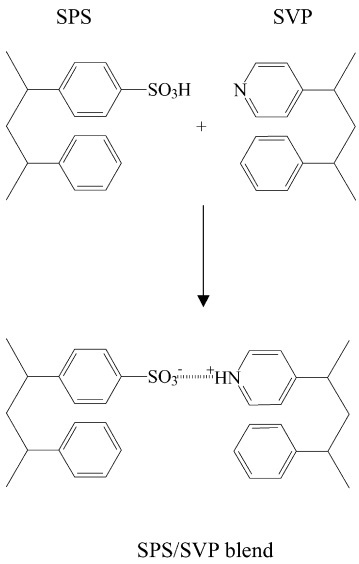

Fig. 1. Schematic illustration indicating chemical structures of polymers and the formation of intermolecular ion–ion interaction (ionic cross-links).

et al. [17]. The starting polymer was polystyrene (PS) having a molecular weight of 4.0×10^5 g/mol. After the sulfonation reaction was terminated by the addition of methanol, polymer (acid form) was recovered by steam stripping in boiling water. After being dried in air for at least 3 days, the polymer was dissolved in a solvent mixture, benzene/methanol (90/10: v/v), and freeze-dried, followed by vacuum drying at room temperature for at least 1 week. The acid contents of the sulfonated PS samples were determined by conductometric titration of the sulfonic acid groups in DMF solution using a standard methanolic sodium hydroxide solution. The details of the preparation and characterization of SPS polymers are described elsewhere [18].

Poly(styrene-*co*-4-vinylpyridine) (SVP) was made by radical bulk copolymerization of styrene with 4-vinylpyridine using benzoyl peroxide (BPO) as an initiator [19]. The concentration of the initiator was 1.56×10^{-3} mol/l. Polymerization was carried out at 60 °C for 16 h to achieve about 10% conversion. Polymer was recovered by precipitating the 5 wt% polymer solution (in toluene) into 10 volumes of methanol under rapid stirring. Precipitated white polymer strands were broken into fine pieces by using a blender. Then, the polymer was filtered under suction and dried in a vacuum oven at 70 °C for 4 days. The degree of polymerization of the polymer was estimated to be about 1.8×10^3 by calculation using the concentration of the initiator. The content of pyridine (Py) groups in the copolymer was determined by using an FTIR calibration curve on poly(4-vinylpyridine) (PVP)/polystyrene (PS) mixture. The calibration curve was obtained as follows: the absorbance spectra of a series of mixtures of PVP/PS with various known PVP contents (< 15 mol%) were obtained, and the characteristic bands for Py and for styrene, St, were identified. Here, we chose the peak at 1558 cm^{-1} for Py and the peak at 1873 cm^{-1} for St. According to the Beer–Lambert law, the following relationship can be obtained [20],

$$A_{1558}/A_{1873} = (\varepsilon_{Py}/\varepsilon_{St})(c_{Py}/c_{St}) \quad (1)$$

Here, A_i is the absorbance at i cm^{-1}, obtained from a peak area. ε_{Py} and ε_{St} represent molar absorptivities of pyridine and styrene, respectively, and c_{Py} and c_{St} are the concentrations (mol/l) of the Py and St in the mixture (PVP/PS). According to Eq. (1), plotting A_{1558}/A_{1873} as a function of molar ratio, c_{Py}/c_{St}, gives a straight line. This was indeed the case for our samples and the line is considered to be a calibration curve (not shown). The value of absorptivity ratio, $\varepsilon_{Py}/\varepsilon_{St}$, was determined from the slope of the straight line as 4.69 from our measurements. When the spectrum of SVP of unknown Py content was measured, its Py content ($= c_{Py}/(c_{Py} + c_{St})$) was calculated from the c_{Py}/c_{St} value, which was obtained from the calibration curve by using a measured A_{1558}/A_{1873} value.

Acid contents of SPS and Py contents of SVP are summarized in Table 1 with the nomenclatures used in this study.

2.2. Blend preparation

The SPS and SVP copolymers were dissolved separately in tetrahydrofuran (THF) (4 wt%), and the solutions were mixed by dropwise addition under vigorous stirring. Blends were prepared so as to contain stoichiometric amounts of interacting groups. Mixing was occasionally accompanied by the formation of gel, which would hinder stirring by a magnetic bar. Hence, stirring was continued by manually swirling the solution for an additional 30 min. The mixture was then stirred with a magnetic bar overnight.

2.3. FTIR spectroscopy

Thin films for FTIR spectroscopy were prepared by casting the solution onto an aluminum foil. When gel formed, thin films were prepared by spreading the gel on the aluminum foil. The thickness of the thin films was ca. 15 μm. Cast films were dried in vacuum oven at 70 °C for 3 days. FTIR spectra were obtained by using a reflection mode with 50 scans and 4 cm^{-1} resolution on a Mattson CYGNUS 100 FTIR spectrometer.

2.4. Transmission electron microscopy (TEM)

Thin film specimens for TEM observation were prepared by solution casting on glass microscope slides [7,21], a somewhat similar procedure to that used by Lauterwasser and Kramer [22]. When gel was formed, the gel was used to make thin film specimens by spreading the gel on glass slides. The slides were then dried in a bell jar, in which a container of the solvent was placed to decrease evaporation rate. The films were cut into small squares (2 × 2 mm) with

Table 1
Nomenclatures and characteristics of the blends and their component polymers

Blend sample	Poly(styrene-*co*-styrenesulfonic acid)	Acid Content (mol%)[a]	Polyl(styrene-*co*-4-vinyl-pyridine)	Pyridine content (mol%)[b]
PS		0		0
SPS3/SVP3	SPS3	2.4	SVP3	3.0
SPS4/SVP5	SPS4	3.6	SVP5	4.7
SPS6/SVP7	SPS6	5.3	SVP7	6.7

[a] Determined by conductometric titration.
[b] Determined by IR.

a razor blade and floated off the glass slides onto distilled water. The pieces of a polymer film were then picked up on copper grids and dried under vacuum at room temperature for at least 3 days. The thickness of the films was kept constant by choosing pieces with the same color: dark gold films with a thickness of around 1500 Å [7]. Thin film specimens clamped in a folding copper grid, were deformed under simple tension by stretching the grid. The induced deformation modes of the strained polymer specimens were maintained by the plastically deformed copper grid, and were observed with a transmission electron microscope (JEM-100CXII) operated at an accelerating voltage of 100 kV.

3. Results and discussion

3.1. FTIR spectroscopy

Fig. 2 shows the spectra of PS, SPS6, SVP7, and a blend, SPS6/SVP7. Comparing the spectrum of SPS6 [spectrum (b)] with that of PS [spectrum (a)], it is seen that identification of the sulfonic acid IR bands is difficult, because a number of absorbencies from polystyrene overlap with those from sulfonic acid. However, the changes of intensity and breadth of the bands can still be noted in a few bands: e.g. the bands at 1364, 1178 and 907 cm^{-1} in the SPS6 are more intense than the corresponding bands in PS. According to the literature [23,24], the absorption bands of asymmetric and symmetric stretching of the O=S=O in $-SO_3H$ groups lie around 1350 and 1170 cm^{-1}, respectively. The absorption band of the stretching vibration of the S–O(H) in $-SO_3H$ groups lies around 907 cm^{-1}. Therefore, the changes of bands at 1364, 1178 and 907 cm^{-1} may be due to contributions from the $-SO_3H$ groups. It is also noteworthy that in the spectrum of SPS6 the absorption bands of either hydrated sulfonic acid or $-SO_3^-$, which are expected to exhibit peaks at around 1140 and 1200 cm^{-1}, due to symmetric and asymmetric stretching vibration of $-SO_3^-$, respectively [23], have not been observed.

Comparison of the spectrum of the SVP7 [spectrum (c)] with that of PS [spectrum (a)] shows clearly that two bands

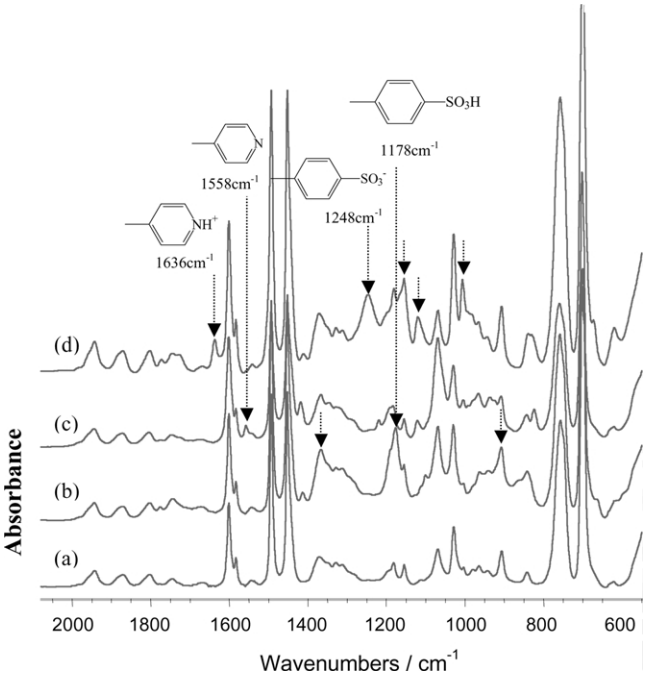

Fig. 2. FTIR absorbance spectra: (a) PS; (b) SPS6; (c) SVP7; (d) SPS6/SVP7 blend.

at 1558 and 1414 cm^{-1} appear only in the spectrum of SVP. Moreover, the intensities of these two bands are proportional to the content of pyridine in the SVP copolymers. These two bands can be assigned to the pyridine ring stretch vibration [24]. When SVP was blended with SPS, the absorption band at 1558 cm^{-1} nearly disappeared, while a new peak at 1636 cm^{-1} emerged as shown in spectrum (d) in Fig. 2. This new peak has no counterpart in SPS. Furthermore, the intensity of this new peak increased with the functionality level of the blends, as can be seen from Fig. 3. Hence, it can be concluded that the appearance of this new peak is related to the interaction between SPS6 and SVP7 upon blending. According to previous studies [15,20], this peak can be assigned to a ring vibration of the pyridinium cations, which were produced through proton transfer from the sulfonic acid groups to the pyridine groups.

In the spectrum of the SPS/SVP blend, another new peak appeared at 1248 cm^{-1}. This peak is particularly evident, since there is no counterpart in either the SVP spectrum or the SPS spectrum. In addition, the peak at 1158 cm^{-1} in the blend is stronger than the sum of absorbances of SPS and SVP at the same wave number. According to Zundel [23], the absorption bands at 1248 and 1158 cm^{-1} can be assigned to the absorption arising from the asymmetric stretching of the $-SO_3^-$ anions. In the spectrum of the SPS/SVP blend, one can find that the peaks at 1119 and 1007 cm^{-1} are also much stronger than the sum of SPS and SVP absorbances at the corresponding wave numbers. The absorption band at 1119 cm^{-1} may include the contribution from the symmetric stretching vibration of the $-SO_3^-$ anions, while the absorption at 1007 cm^{-1} may include the contribution from in-plane bending vibration of a

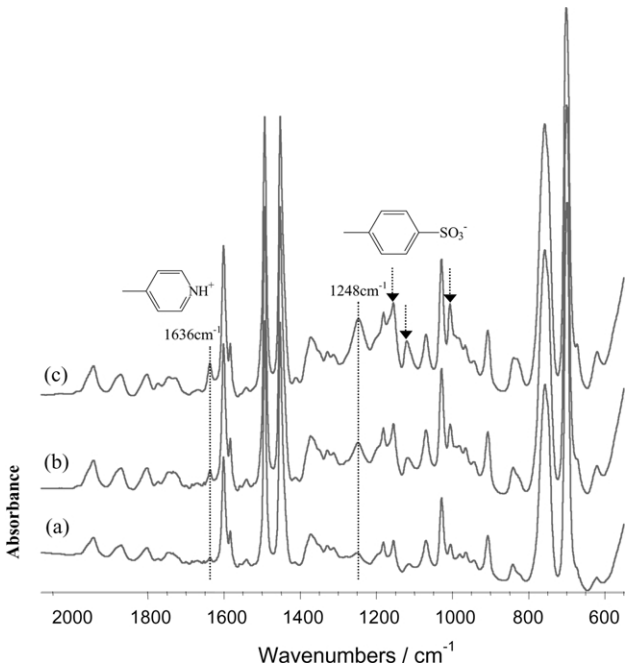

Fig. 3. FTIR absorbance spectra of SPS/SVP blends: (a) SPS3/SVP3; (b) SPS4/SVP5; (c) SPS6/SVP7.

disubstituted benzene ring with the substitute of $-SO_3^-$ structure. From Fig. 3, it can be seen that the intensities of all these peaks (at 1248, 1158, 1119 and 1007 cm^{-1}) are proportional to the functionality level. Hence, it can be concluded that sulfonate anions ($-SO_3^-$) were formed upon blending.

As discussed above, the formation of sulfonate anions and pyridinium cations upon blending due to proton transfer has been confirmed by their characteristic absorption bands. The next question is the location of sulfonate anions and pyridinium cations in the blend: whether the sulfonate anions and pyridinium cations in the blend are separated or in close proximity. We may obtain the answer from analysis of the position of absorption bands corresponding to the asymmetric stretching of $-SO_3^-$ anions [23]. If the $-SO_3^-$ anions are isolated from their surrounding, the charge is almost uniformly distributed among three S⋯O bonds, so that the mesomerism is very strong and three almost identical S⋯O bonds are present. In this case, the $-SO_3^-$ anion has a pyramidal structure; i.e. it possesses C_{3v} 'local' symmetry. The asymmetric stretch vibration of a group with C_{3v} local symmetry is doubly degenerate. Thus, the absorption due to the asymmetric stretching of $-SO_3^-$ anions in this case appears as only one absorption band around 1200 cm^{-1}. On the other hand, if cations are attached to the $-SO_3^-$ anions, the latter are somewhat polarized by the electrostatic field of their cations, the mesomeric bond resonance in these anions is disturbed, and C_{3v} local symmetry is changed to C_s symmetry. This, in turn, removes the degeneracy of the asymmetric stretching vibration of $-SO_3^-$ anions. Therefore, it gives rise to the splitting of the absorption band for the asymmetric stretching of $-SO_3^-$ anions, one band with higher wave number always lying above 1200 cm^{-1}, and the other band with lower wave number below 1200 cm^{-1}. Furthermore, it has been found that the degree of the splitting of the band is dependent on the strength of the electrostatic field of their cations; i.e. the splitting of the band near 1200 cm^{-1} is greater, when the field of the cation near the anion is stronger [23]. In the present case, we observe two bands at 1248 and 1155 cm^{-1} in the blends, which are attributed to the asymmetric stretching of the $-SO_3^-$ anions. Therefore, we conclude that $-SO_3^-$ anions and pyridinium cations are attached to one another in the blends to form ion pairs, which give rise to the formation of (ionic) cross-links of the polymer chains. The splitting in the present case is 93 cm^{-1}, which is much larger than the splitting found for the Na^+ salt of poly(styrenesulfonic acid) (splitting of 38 cm^{-1}) and for the Ca^{2+} salt of poly(styrenesulfonic acid) (splitting of 54 cm^{-1}) [23]. This means that the strength of the electrostatic interactions in ion pairs of sulfonate anions with counterions has the following order: pyridinium cation/sulfonate anion ion pairs > $-SO_3^-/Ca^{2+}$ ion pairs > $-SO_3^-/Na^+$ ion pairs.

To estimate as to what extent anion/cation pair interactions take place upon blending, quantitative analysis can be made by using the characteristic pyridinium cation peak at 1636 cm^{-1} and the pyridine peak at 1558 cm^{-1}. We start from the following equation,

$$c_{Py^+} + c_{Py} = c_{Py}^0 \tag{2}$$

where c_{Py^+} and c_{Py} represent the concentrations (mol/l) of pyridinium cation and residual pyridine upon blending, respectively, and the c_{Py}^0 is the initial concentration of pyridine (before proton transfer occurred). According to the Beer–Lambert law, Eq. (2) may be converted to [15]

$$\frac{A_{1636}/A_{1873}}{\varepsilon_{Py^+}/\varepsilon_{St}} + \frac{A_{1558}/A_{1873}}{\varepsilon_{Py}/\varepsilon_{St}} = \frac{c_{Py}^0}{c_{St}} \tag{3}$$

where ε_{Py^+} represents the molar absorptivity of the pyridinium cation in styrene, and c_{St} is the total concentration (mol/l) of styrene in the mixture.

Rearrangement of Eq. (3) gives

$$\frac{A_{1636}/A_{1873}}{c_{Py}^0/c_{St}} = \frac{\varepsilon_{Py^+}}{\varepsilon_{St}} - \left(\frac{\varepsilon_{Py^+}}{\varepsilon_{Py}}\right)\frac{A_{1558}/A_{1873}}{c_{Py}^0/c_{St}} \tag{4}$$

Plotting $(A_{1636}/A_{1873})/(c_{Py}^0/c_{St})$ against $(A_{1558}/A_{1873})/(c_{Py}^0/c_{St})$ should yield a straight line whose slope is $-(\varepsilon_{Py^+}/\varepsilon_{Py})$ and the intercept is $(\varepsilon_{Py^+}/\varepsilon_{St})$. Fig. 4 shows such a plot. From the slope and the intercept, absoptivity ratios to styrene, of pyridinium cation and of pyridine, i.e. $(\varepsilon_{Py^+}/\varepsilon_{St})$ and $(\varepsilon_{Py}/\varepsilon_{St})$, were calculated as 12.0 and 4.53, respectively. Even though only three points measured from the blends are plotted in Fig. 4, the absorptivity ratio of Py to styrene obtained here ($\varepsilon_{Py}/\varepsilon_{St} = 4.53$) is in good agreement with the previous value ($\varepsilon_{Py}/\varepsilon_{St} = 4.69$) obtained from the polymer mixture, PVP/PS. Thus, it is believed that the values of

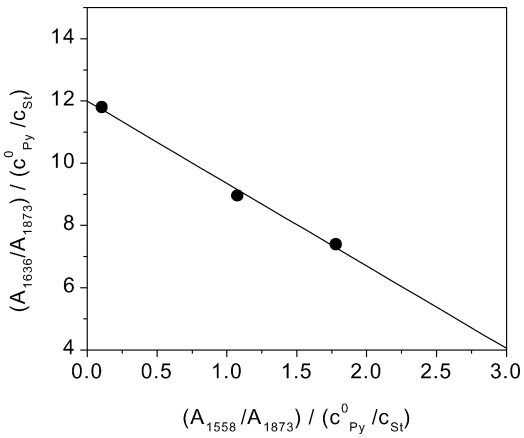

Fig. 4. A plot of FTIR data according to Eq. (4) for the evaluation of the absorption coefficient of pyridinium cation.

absorptivity ratios obtained from Fig. 4 are accurate enough to estimate the contents of pyridinium cation. The estimated ion contents (mol%) in the blends are summarized in Table 2. The protonation efficiency, defined as the number ratio of protonated Py units to Py before blending, is high [20]; for example, over 80% for the SPS6/SVP7 blend determined in this work.

3.2. Deformation behavior of SPS and SVP

Fig. 5 shows low magnification TEM micrographs of strained thin films for PS, SPS6 and SVP7, respectively. The micrographs from the strained samples of SPS and SVP with lower functionalities (not shown here) are similar to those shown in Fig. 5. It can be seen that both the SPS6 and SVP7 samples deform only by localized crazing and most of the crazes, which grow in a direction perpendicular to the applied stress axis, tend to be long and straight. This deformation behavior is basically identical to that observed in the PS homopolymer sample shown in Fig. 5(a). Fig. 6 shows a typical craze microstructure found in SPS, which is similar to that found in SVP. Crazes consist of highly extended fibrillar elements interspersed with voids. They contain a thin central section, a so-called midrib, with lower fibril density, and the craze-bulk interfaces are relatively sharp [2,3]. Also, the craze tapers at the end to a relatively fine point. In general, SPS and SVP samples are found to have identical deformation behavior to that found in PS. This indicates that the introduction of a small amount of functional groups (either sulfonic acid or pyridine) into PS does not change the basic deformation behavior, although SPS polymers may contain hydrogen bonding between sulfonic acid groups.

3.3. Deformation behavior of SPS/SVP blends

Fig. 7 shows TEM micrographs of strained thin films of the SPS3/SVP3 blend. From the micrograph with low magnification (Fig. 7(a)), one can see that there are many shorter crazes in this blend, in contrast to PS homopolymer, SPS, or SVP in which most of the crazes span the grid bars. The micrograph with high magnification (Fig. 7(b)) shows that crazes have a tendency to bifurcate and extend in directions other than perpendicular to the applied stress. This suggests that some shear deformation may also be present, resulting in both shorter crazes and more resistance to fracture [2,3,25,26].

The change of deformation behavior is more evident when the content of interacting groups in the SPS/SVP blends increases further. Fig. 8 shows a TEM micrograph of a strained thin film of the SPS4/SVP5 blend. In this sample, even though crazing is still a dominant deformation mode, one can observe formation of short shear deformation zones between craze tips. These shear deformation zones stabilize the polymer against rapid craze growth and result in the suppression of longer crazes [2,3].

The shear deformation becomes more significant in the SPS6/SVP7 blend than in the SPS4/SVP5 blend, as shown in Fig. 9. Most crazes do not taper to a sharp tip but are blunted by shear deformation zones. The craze region tends to become thicker and much shorter than in the samples having fewer interacting groups.

It can be concluded that deformation behavior in the blends changes from crazing only to crazing plus shear deformation, with an increasing degree of shear deformation, as the interacting group content increases. Our FTIR results have shown that $-SO_3^-$ anions and pyridinium cations in the SPS/SVP blends are attracted to each other to form ion pairs, which give rise to the ionic cross-links between polymer chains. These ion pairs are the only difference between the blends and their parent polymers (PS). Hence, the change of deformation behavior in the present system is believed to arise from the formation of ionic cross-links in the blends.

Table 2
Strand densities and deformation modes of SPS/SVP blends

Blends	Ion content in the blend[a] (mol%)	Ionic strand density (ν_i) (10^{25} chains/m^3)	Total strand density (ν) (10^{25} chains/m^3)	Deformation mode
PS	0	0	3.3	Crazing only
SPS3/SVP3	2.0	12	15	Crazing plus shear (reflected in bifurcation)
SPS4/SVP5	3.1	18	21	Crazing plus shear (small)
SPS6/SVP7	5.8	34	37	Crazing plus shear (diffuse and extensive)

[a] Determined by IR.

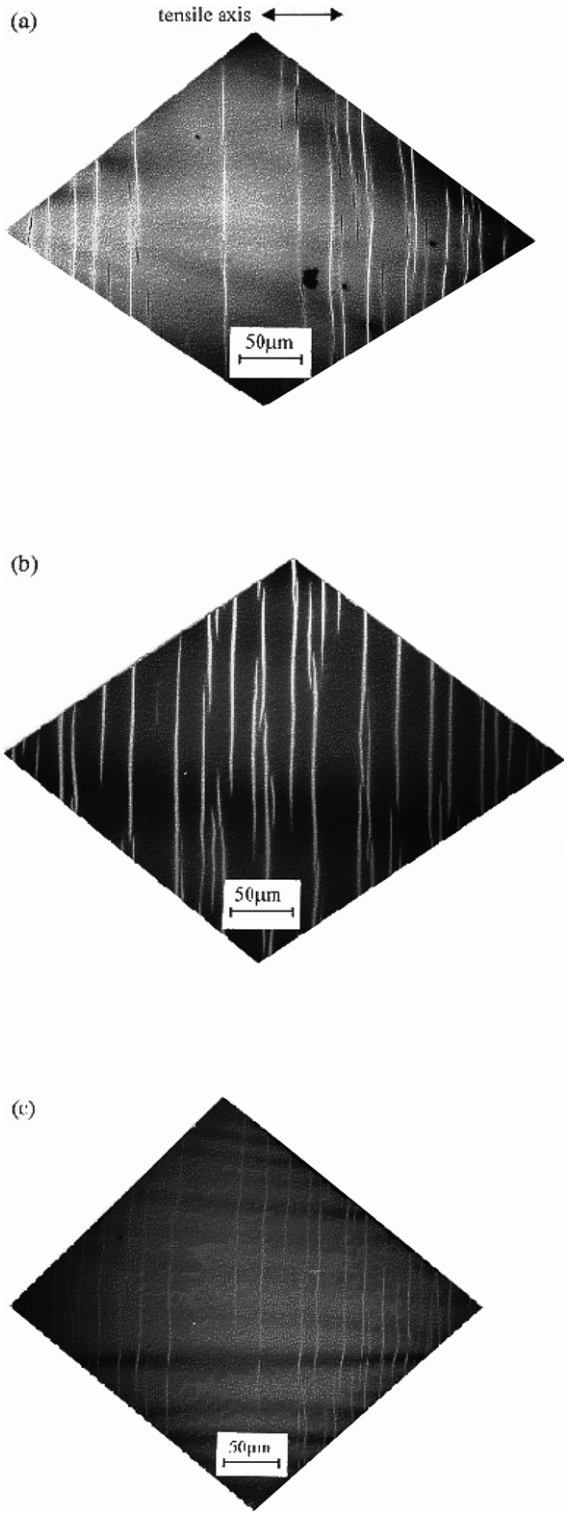

Fig. 5. TEM micrographs with low magnification: (a) PS; (b) SPS6; (c) SVP7.

The concept of a network strand density is helpful to understand the changes that occurs in the deformation behavior. Since ionic cross-links provide somewhat similar effects to covalent cross-links or physical entanglements, we can define an ionic strand density, ν_i, in a fashion similar to

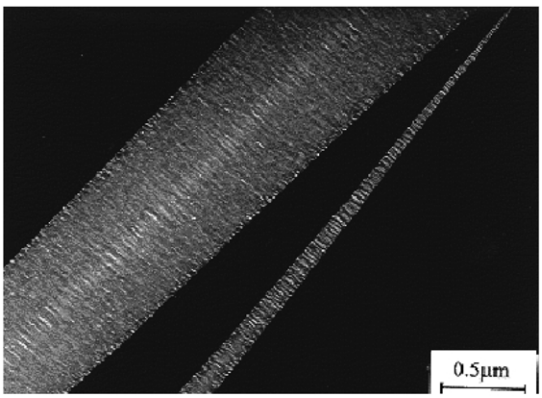

Fig. 6. TEM micrograph showing a typical craze microstructure observed for SPS.

the physical entanglement strand density. For linear polymers, such as homopolymers and copolymers, the strand density, ν_e, due to physical entanglement, is defined as [2,3].

$$\nu_e = \rho N_a / M_e \tag{5}$$

where ρ is the polymer density (kg/m^3), N_a is the Avogadro's number and M_e is the entanglement molecular weight (kg/mol) (see Fig. 10(a)).

In a similar fashion, the ionic cross-link strand density

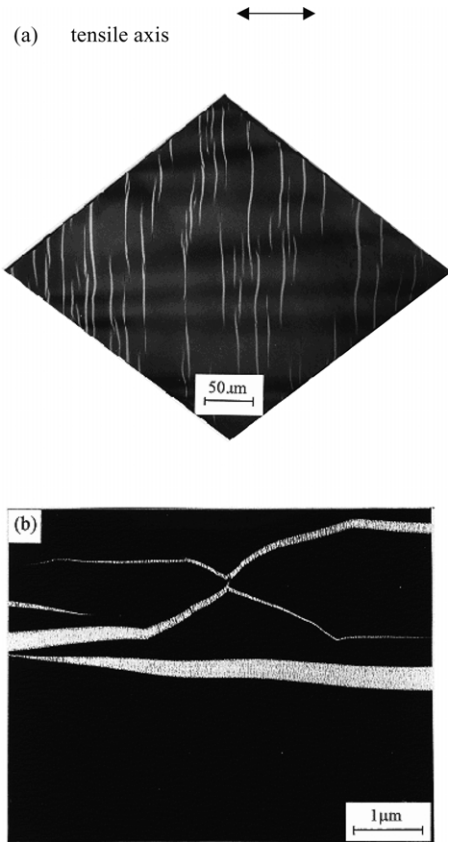

Fig. 7. TEM micrographs of strained thin films of SPS3/SVP3 blend: (a) low magnification; (b) high magnification showing bifurcated craze microstructure.

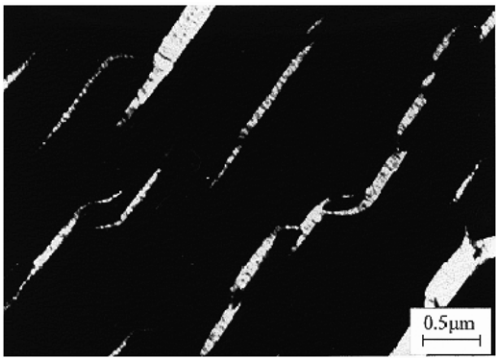

Fig. 8. TEM micrograph of strained thin films of SPS4/SVP5 blend showing crazes plus shear deformation.

may be evaluated by

$$\nu_i = \rho N_a / M_i = f \rho N_a / M_0 \quad (6)$$

where M_i is the average molecular weight between ionic groups (see Fig. 10(b)), f is the ion content (mole fraction), and M_0 is the repeat unit molecular weight. By combining these two strand densities, the (apparent) total strand density may be obtained as

$$\nu = \nu_e + \nu_i \quad (7)$$

Here, ν represents the total (network) strand density, defined as the number of strands (molecular chains separated by two junction points that include physical entanglement and ionic cross-links) per unit volume. Such relations have been used for describing the deformation modes of covalently cross-linked polymers by using ν_x (covalent cross-link strand density) instead of ν_i by Henkee and Kramer [5]. The formation of ionic cross-links can raise the strand density as well.

The ionic strand density and the (apparent) total strand density for each sample in our experiment can be estimated by Eqs. (5)–(7), based on the assumptions that all ion pairs participate in creating ionic cross-links and that the ionic cross-links are comparable to covalent or entanglement

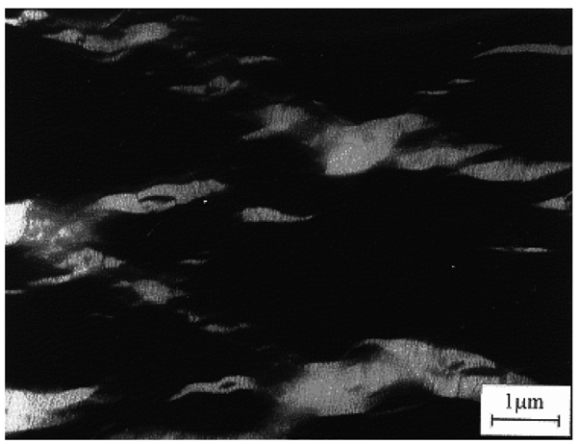

Fig. 9. TEM micrograph of strained thin films of SPS6/SVP7 blend showing crazes that interact with and are blunted by shear deformation.

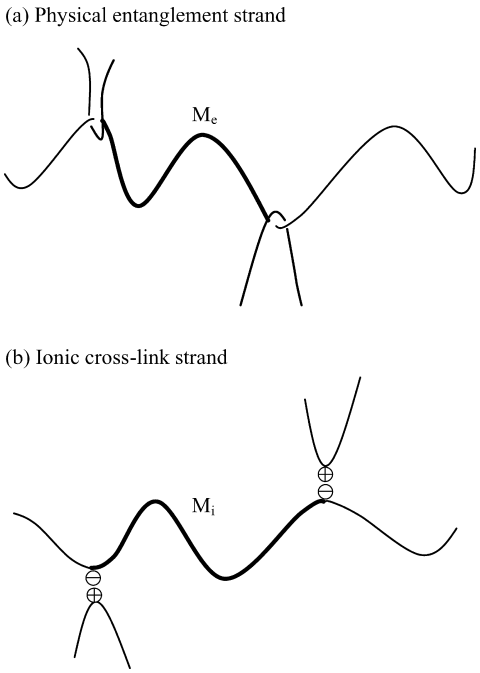

Fig. 10. Schematic illustration indicating (a) a physical entanglement strand and (b) an ionic cross-link strand.

cross-links (at temperature well below T_g). Results are summarized in Table 2, and the observed deformation mode in the SPS/SVP blends for each sample is also included in Table 2. As seen from Figs. 7–9 and Table 2, shear deformation is more extensive for the SPS6/SVP7 blend, smaller but clearly seen for the SPS4/SVP5 blend, but not clearly visible for the SPS3/SVP3 blend, although the complex craze pattern suggests that some shear nature is present. Thus, it is not unreasonable to assume that the transition of deformation mode from crazing only to crazing plus some shear deformation occurs for the SPS3/SVP3 sample having a total strand density of ca. 15×10^{25} chains/m^3.

This value is about four times of that for covalently cross-linked PS system, in which the transition of deformation behavior from crazing only to crazing plus shear deformation occurs at a strand density of 4×10^{25} chains/m^3, as reported by Henkee and Kramer [3,5]. This result may be understood by the following considerations. Although ionic cross-linking does provide somewhat similar effects to covalent cross-linking, such as a shift of T_g to higher temperatures, ionic cross-links are not as strong and stable as covalent cross-links. For example, ionic cross-links can be overcome at high temperature. The dissociation of ion pairs is expected to be easier than chain scission, which involves covalent bond breakage. In other words, the energy needed to break one ionic bond is lower than that to break one covalent bond. Therefore, as compared with the strands due to covalent cross-links or physical entanglements (at temperature well below T_g), the strands due to ionic cross-links may contribute less to the surface energy that is needed for the formation of the craze (fibril) surface

during crazing. This surface energy is a key parameter in determining as to when crazing becomes unfavorable as compared to shear deformation. Hence, for the SPS/SVP blends, the effective strand densities will be smaller than the values (shown in Table 2), based on the assumption that ionic cross-links are comparable to covalent cross-links.

There is another point to be considered. As Berger and Kramer [26] have pointed out, the strand density value of 4×10^{25} chains/m^3, where the transition of deformation mode in polymers occurred, was observed for one particular method of film preparation, for one film thickness, and for one particular stress condition. They found that the value of strand density at which the deformation mode changed from crazing only to crazing plus shear deformation for cross-linked PS shifted to 9×10^{25} chains/m^3 if the PS film was physically aged before crazing at 75 °C for 10–12 h. If this is the case, the difference between the value of strand density at which the transition of deformation mode occurs in the present case and the value for covalently cross-linked PS is not as large as noted here, based on a value of 4×10^{25} chanis/m^3 for the covalently cross-linked PS.

It might be more useful to compare the values of apparent strand densities at which the transition of deformation occurs in the present case to that in the case of SPS ionomers with metallic counterions (e.g. Na-SPS or Ca-SPS), since sample preparation and testing conditions of these systems are similar to the present case [6,9]. We have reported that shear deformation develops in addition to crazing as the ion content reaches about 6 mol% or above in Na-SPS ionomers [6,9,18,21]. If we assume that the transition of deformation behavior from crazing only to crazing plus shear deformation occurs at 6 mol%, the corresponding ionic strand density, ν_i, is 36×10^{25} chains/m^3. In the case of Ca-SPS ionomers [6], both crazing and shear modes developed at an ion content of 4.1 mol% and the corresponding ionic strand density, ν_i, is 25×10^{25} chains/m^3. These results indicate that ionic cross-links due to presence of pyridinium cation/sulfonate anion groups have a stronger effect on inducing the transition of deformation behavior than ionic cross-links via $-SO_3^-/Na^+$or $-SO_3^-/Ca^{2+}$ ion pairs. The effectiveness for inducing the deformation mode transition may be summarized as follows: direct ionic cross-links (pyridinium cation/sulfonate anion) > ionic cross-links with doubly ionized Ca^{2+} ion > ionic cross-links with singly ionized Na^+ ion. This result can be understood from consideration of the strength of the electrostatic (anionic/cationic) interactions in ion pairs: as discussed in the FTIR study, where the order is the same as the order for the deformation mode transition.

In summary, our studies have shown that multiple-deformation behavior involving crazing plus shear deformation can be achieved by introducing direct ionic cross-links into polymers. The multiple-deformation behavior is important in increasing toughness of polymers, as it limits the growth and breakdown of crazes, prevents premature crack initiation, and favors larger plastic strains and increased energy absorption. Our results suggest that bulk mechanical properties may also be enhanced by the introduction of intermolecular ionic cross-links (bonding) [27], even though our observations of deformation behavior were obtained on thin films under plane stress conditions, while observations on bulk specimens are obtained under plane strain conditions. Enhanced bulk mechanical properties have been reported for glassy ionomers, in which similar changes in the deformation mode have been made [6,9].

4. Conclusions

To study the effects of intermolecular ionic interactions and ionic cross-links on deformation behavior, SPS/SVP blends have been used as a model system. In such blends, two functional groups, 4-vinylpyridine and sulfonic acid, are introduced separately onto polystyrene backbone chains. FTIR studies have shown that pyridinium cations and sulfonate anions are formed by proton transfer from sulfonic acid groups to pyridine groups upon blending. The FTIR data also indicate that pyridinium cations and sulfonate anions formed upon blending are attached closely to each other to form intermolecular ionic cross-links; and that the strength of electrostatic (cationic/anionic) interaction in pyridinium cation/sulfonate anion ion pairs is stronger than that in either $-SO_3^-/Ca^{2+}$ ion pairs or $-SO_3^-/Na^+$ ion pairs.

The introduction of the intermolecular ionic cross-links via pyridinium cation/sulfonate anion ion pairs effectively modifies the deformation behavior of SPS/SVP blends. TEM observations of strained thin films of PS, SPS and SVP showed that these polymers deformed only by crazing; but, in the SPS/SVP blends the deformation mode changed from crazing only to crazing plus shear deformation at an ion content in the blend of around 2.0 mol%. It is believed that the effective strand density is increased upon introduction of ionic cross-links, thereby allowing shear deformation to compete with crazing. Moreover, it has been found that the ionic cross-links, due to formation of the pyridinium cation/sulfonate anion pairs, are more effective in modifying deformation behavior than those via $-SO_3^-/Ca^{2+}$ or $-SO_3^-/Na^+$ ion pairs.

The achievement of multiple-deformation behavior, involving crazing plus shear deformation, by the introduction of intermolecular ionic cross-links suggests that bulk mechanical properties of polymers may also be enhanced. Thus the mechanical properties of the SPS/SVP blends under plane strain conditions are now under investigation. Initial results indicate that a synergistic enhancement in bulk mechanical properties occurs; i.e. the average values of toughness and tensile strength are higher than values expected based on the rule of mixtures, and values of both properties are increased with the interacting group content. Details of the bulk mechanical properties study are reported in a separate article [27].

Acknowledgements

Acknowledgment is made to the US Army Research Office and to the Donors of the American Chemical Society Petroleum Research Fund for support of this research.

References

[1] Kinloch AJ, Young RJ. Fracture behavior of polymers. New York: Applied Science Publishers; 1983.
[2] Kramer EJ. Adv Polym Sci 1983;52/53:1.
[3] Kramer EJ, Berger LL. Adv Polym Sci 1990;91/92:1.
[4] Bucknall CB. In: Paul DR, Newman S, editors. Polymer blends. New York: Academic Press; 1978.
[5] Henkee CS, Kramer EJ. J Polym Sci, Polym Phys Ed 1984;22:721.
[6] Hara M, Sauer JA. J Macromol Sci, Rev Macromol Chem Phys 1994; C34:325.
[7] Ma X, Sauer JA, Hara M. Macromolecules 1995;28:5526.
[8] Ma X, Sauer JA, Hara M. Polymer 1996;37:4739.
[9] Hara M, Sauer JA. In: Salamone J, editor. Polymeric materials encyclopedia. New York: CRC Press; 1996. p. 3465.
[10] Eisenberg A, King M. Ion-containing polymers. Academic Press: New York; 1977.
[11] Smith P, Hara M, Eisenberg A. In: Ottenbrite RM, Utracki LA, Inoue S, editors. Current topics in polymer science. New York: Hanser Publishers; 1987. p. 256.
[12] Zhang X, Eisenberg A. J Polym Sci, Part B Polym Phys 1990;28:1841.
[13] Natansohn A, Eisenberg A. Macromolecules 1987;20:323.
[14] Douglas EP, Sakurai K, MacKnight WJ. Macromolecules 1991;24: 6776.
[15] Sakurai K, Douglas EP, MacKnight WJ. Macromolecules 1992;25: 4506.
[16] Douglas EP, Waddon AJ, MacKnight WJ. Macromolecules 1994;27: 4344.
[17] Makowski HS, Lundberg RD, Sighal GH. US Patent 3,870,841; 1975.
[18] Bellinger M, Sauer JA, Hara M. Macromolecules 1994;27:1407.
[19] Gauthier S. PhD Thesis, McGill University, Montreal; 1985.
[20] Smith P, Eisenberg A. Macromolecules 1994;27:545.
[21] Hara M, Jar P. Macromolecules 1988;21:3187.
[22] Lauterwasser BD, Kramer EJ. Philos Mag 1979;A39:469.
[23] Zundel G. Hydration and intermolecular interaction. New York: Academic Press; 1969.
[24] Colthup NB, Daly LH, Wiberley SE. Introduction to infrared and raman spectroscopy, 2nd ed. New York: Academic Press; 1975.
[25] Donald AM, Kramer EJ, Kambour RP. J Mater Sci 1982;17:1739.
[26] Berger LL, Kramer EJ. J Mater Sci 1988;22:1046.
[27] Chen W, Sauer JA, Hara M. Polymer 2003: in press.